Time-independent and Time-dependent Seismic Hazard Assessment for the State of California: Uniform California Earthquake Rupture Forecast Model 1.0

Mark D. Petersen,[1] Tianqing Cao,[2] Kenneth W. Campbell,[3] and Arthur D. Frankel[1]

INTRODUCTION

Ground-shaking hazard maps based on sound earth-science research are effective tools for mitigating damage from future earthquakes. Assuming that future earthquakes will occur on active faults or near previous events and that the ground shaking from these events will fall within the range of globally recorded ground motions leads to probabilistic hazard maps that predict ground-shaking potential across a region. Developing hazard and risk maps requires technical interactions between earth scientists and engineers to estimate the rate of potential earthquakes across a region, quantify likely ground-shaking levels at a site, and understand how buildings respond to strong ground shaking. For the past 25 years the U.S. Geological Survey (USGS) and California Geological Survey (CGS) have cooperated with government officials and professional organizations to incorporate hazard maps and other hazard products in public and corporate documents such as building codes, insurance rate structures, and earthquake risk mitigation plans (Algermissen and Perkins 1982; Frankel *et al.* 1996, 2002; Petersen *et al.* 1996).

Because these hazard products are used in making public-policy decisions, it is essential that the official USGS-CGS hazard models reflect the "best available science." This qualification is also required by the statute that regulates the California Earthquake Authority, which provides most earthquake insurance in the state. To adequately represent the "best available science," hazard maps need to be updated regularly to keep pace with new scientific advancements. The methodologies, computer codes, and input data used in developing these products need to be openly available for review and analysis. Input parameters and codes for current hazard maps may be obtained at http://earthquake.usgs.gov/hazmaps and http://www.consrv.ca.gov/cgs. At these Web sites a user may access documentation that describes methodologies and parameters, a relational database and tables that contain explanations of how the fault parameters and uncertainties were chosen, interactive tools that allow the user to view hazard map information and to disaggregate the hazard models, and Web interfaces that present building code design values at a latitude and longitude or zip code of interest.

The USGS has historically developed time-independent models of earthquake occurrence that are based on the assumption that the probability of the occurrence of an earthquake in a given period of time follows a Poisson distribution. Probabilities calculated in this way require only knowledge of the mean recurrence time. Results of these calculations do not vary with time (*i.e.*, results are independent of the time since the last event) and are a reasonable basis for provisions guiding earthquake resistance in building codes and long-term mitigation strategies.

In contrast, time-dependent models of earthquake occurrence are based on the assumption that the probability of occurrence of an earthquake in a given time period follows a renewal model, *i.e.*, a log-normal, Brownian passage time (BPT), or other probability distribution in which the probability of the event depends on the time since the last event (appendix A). In addition to the mean frequency (or recurrence time) of earthquakes, these models require additional information about the variability of the frequency of events (the variance or standard deviation) and the time of the last event. The time-dependent models are intuitively appealing because they produce results broadly consistent with the elastic rebound theory of earthquakes. The USGS and CGS are beginning to develop these types of hazard products as new geologic and seismic information regarding the dates of previous events along faults becomes available.

In application, both the time-independent and time-dependent models depend on assumptions about the magnitude-frequency characteristics of earthquake occurrence, the simplest of which is the "characteristic earthquake model" in which all large earthquakes along a particular fault segment are assumed to have similar magnitudes, average displacements, and rupture lengths (Schwartz and Coppersmith 1984). More complicated models

1. U.S. Geological Survey, Denver.
2. California Geological Survey.
3. EQECAT, Inc.

include Gutenburg-Richter magnitude-frequency distributions and multisegment ruptures (Gutenberg and Richter 1944). In as much as time-dependent models require more input parameters and assumptions as contrasted with time-independent models, there is not yet the same degree of consensus about the methods and results for these calculations.

Both time-independent and time-dependent hazard calculations require moment-balanced models that are consistent with the global plate rate models and slip rates determined on individual faults. Geologists can estimate the average slip rates on faults in California from offset geologic features that have been dated using radiometric dating techniques. At sites along some faults, we know the approximate times of past events extending hundreds or thousands of years into the past, but we do not know the magnitudes of or the lengths of faults involved in these past earthquakes. A fundamental constraint that we apply to candidate earthquake occurrence models, commonly called "moment balancing," is the requirement that over the long term the displacements from the earthquakes sum to the observed slip rate all along the fault. Models that permit smaller earthquakes will generally contain more frequent earthquakes to add up to the total slip rate.

In this paper we describe the general characteristics of the time-independent (Poisson) 2002 USGS-CGS California seismic hazard models and develop a time-dependent model—the first version of the Working Group on California Earthquake Probability (WGCEP) uniform California earthquake rupture forecast model (UCERF 1.0). The time-independent and time-dependent hazard maps and hazard curves provide a basis for comparison for the Regional Earthquake Likelihood Models (RELM) presented in this volume and future WGCEP models that will be developed over the next few years. The time-dependent model does not have the same consensus inputs that are incorporated in the standard time-independent model, and so the user should use caution in applying these maps. However, this new model builds on information collected from several WGCEP models (1988, 1990, 1995, 1999, 2003), time-dependent models published by Cramer *et al.* (2000) and Petersen *et al.* (2002), paleoseismic data from Weldon *et al.* (2004), and recent seismicity data. Time-dependent analysis incorporates first-order information on the elapsed time since the last earthquake and should provide a reasonable basis for comparison.

THE 2002 USGS-CGS TIME-INDEPENDENT SEISMIC HAZARD MODEL

The USGS and CGS released California hazard maps in 1996 and 2002 using a probabilistic seismic hazard framework and incorporating information from regional workshops held across the country (Petersen *et al.* 1996; Frankel *et al.* 1996, 2002). The current hazard model is based on fault information, seismicity catalogs, geodetic data, and ground-shaking attenuation relations that were discussed at these workshops. An advisory committee reviewed these models and made recommendations on how the resulting products could be improved.

The 2002 California model incorporates nearly 200 fault sources that generate thousands of earthquake ruptures. It is not possible to describe details of the methodology and fault parameters in the limited space available here. Instead, we refer the reader to published references, data, and products available at http://earthquake.usgs.gov/hazmaps/; http://www.consrv.ca.gov/cgs; Petersen *et al.* 1996; and Frankel *et al.* 1996, 2002, which provide the input parameters and codes needed to reproduce the official hazard model. In the section below we provide only a general description of the methodology, input data, and results.

The known fault sources considered in the model contribute most to the high hazard regions of California (see Petersen *et al.* 1996 deaggregation). Faults are divided into two classes, A-type and B-type. The A-type faults generally have slip rates greater than 1 mm/yr and paleoseismic data that constrain the recurrence intervals of large earthquakes (figure 1). Various editions of the WGCEP report indicate that sufficient information is available for these faults to allow development of rupture histories and time-dependent forecasts of earthquake ruptures. Models are developed using single-segment and multisegment earthquake ruptures as defined by various working groups in northern and southern California.

The B-type faults include all of the other faults in California that have published slip rates and fault locations that can be used to estimate a recurrence interval. To calculate the recurrence, the moment of the characteristic earthquake is divided by the moment rate determined from the long-term fault slip rate to obtain recurrence time. For a few faults we fixed the magnitudes and/or recurrence rate based on historical earthquakes or paleoseismic studies. We used a logic tree to account for epistemic uncertainty in our knowledge of which magnitude-frequency distribution is correct for future earthquakes. In the hazard model a truncated Gutenberg-Richter distribution that spans magnitudes between 6.5 and the characteristic size is weighted one-third and a characteristic distribution defined by a simple delta function is weighted two-thirds. Modeling uncertainties in the characteristic or maximum magnitudes of a fault are accounted for explicitly in the calculation procedure.

In addition to the fault sources, a random source is used to account for earthquakes on unknown fault sources and moderate-size earthquakes on faults. This portion of the model is most important in areas that lack known active faults, but it also contributes significantly to our knowledge of the overall seismicity hazard across the state. The random background source model is based on earthquake catalogs. For the 1996 and 2002 hazard analyses, we developed a statewide earthquake catalog for magnitudes greater than 4 from the late 1700s to 2000 (Petersen *et al.* 1996, Petersen *et al.* 2000; Toppozada *et al.* 2000). This statewide catalog was developed using regional catalogs from the USGS (Menlo Park and Pasadena), California Institute of Technology, University of California-Berkeley, University of Nevada-Reno, and published results on earthquake moment magnitudes. Mine blasts and duplicate earthquakes were removed from the catalog. For the time-independent hazard assessment we considered only independent events; dependent events are not consistent with the assumption of independence

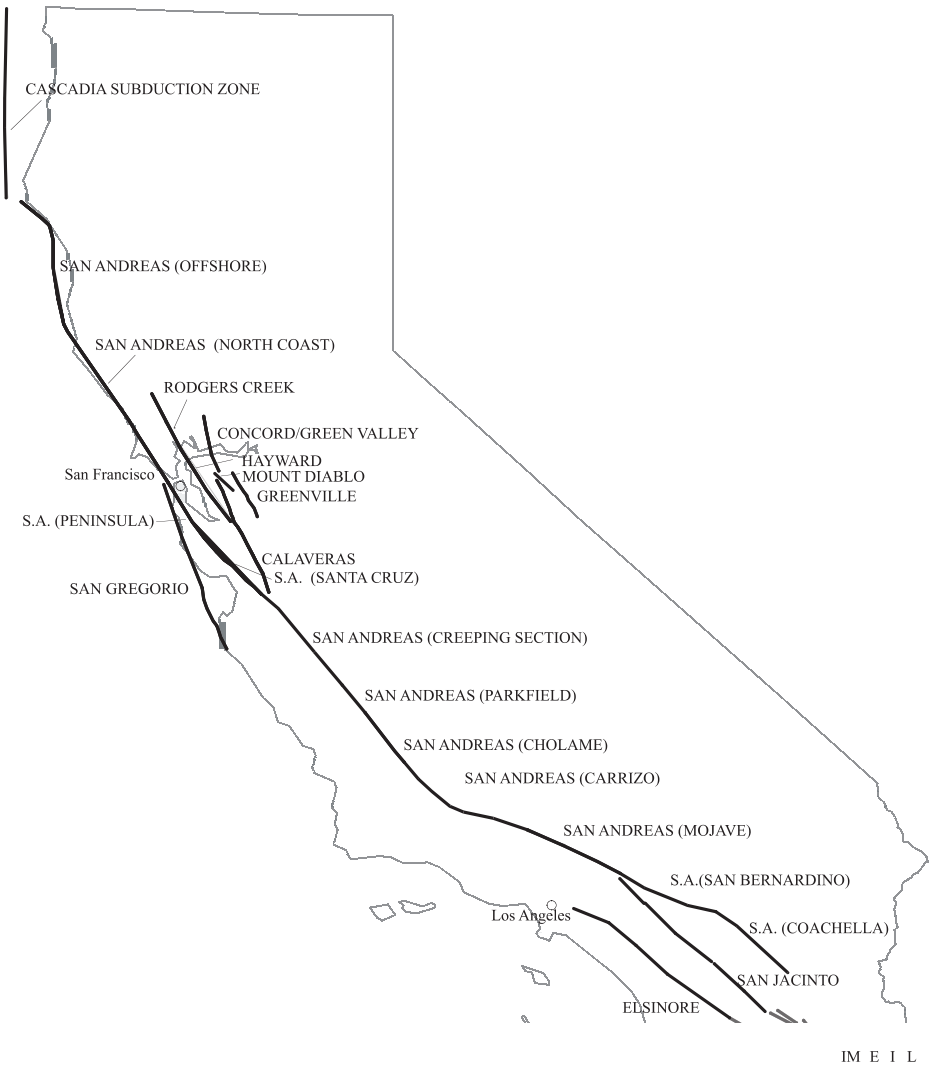

▲ **Figure 1.** Locations and names of A-faults contained in the source model.

in a Poisson process. We applied the algorithm of Gardner and Knopoff (1974) to decluster the catalog, removing aftershocks and foreshocks identified using magnitude and distance criteria. The earthquakes in the catalog are spatially binned over a grid and smoothed using a Gaussian distribution with a 50-km correlation length to obtain the rate of earthquakes in the background model (Frankel 1995). The hazard is then computed by using the rate at each grid node in conjunction with a Gutenberg-Richter magnitude frequency distribution and attenuation relations to obtain the rate of exceedance at each ground-motion level.

In portions of eastern California and western Nevada there are differences between the model rate of earthquakes calculated from the geologic slip rate data and the historic rate of earthquakes from the earthquake catalog (Frankel *et al.* 2002). Recent geodetic data seem to be more consistent with the historic earthquake data, both suggesting higher contemporary strain rates than would be implied from geologic studies. Therefore, in four regions of eastern California and western Nevada we have used the geodetic data to supplement our earthquake fault models, called C-zones. The earthquakes are modeled using geodetically based slip rates that are spread uniformly across a zone and modeled using a Gutenberg-Richter magnitude-frequency distribution. Future research should help delineate the particular faults that are accommodating the observed geodetic strains and determine if recent data reflect the long-term strain rates or if these data are dominated by secular variability.

Once we have quantified the earthquake sources we can apply published empirical attenuation relations to estimate the potential ground-shaking levels from the modeled earthquakes. We have applied four attenuation relations, equally weighted, for coastal California earthquakes (Abrahamson and Silva 1997; Boore *et al.* 1997; Campbell and Bozorgnia 2003; Sadigh *et al.* 1997). For the extensional region we have also applied the attenuation relation of Spudich *et al.* (1999). Ground motions from the Cascadia subduction zone are calculated using the attenuation relations for interface earthquakes of Youngs *et al.* (1997) and Sadigh *et al.* (1997) and for deep intraslab earthquakes of Atkinson and Boore (2003) and Youngs *et al.* (1997). Generally, attenuation relations should be updated when sufficient strong-motion data are recorded that show inconsistencies with the previous relations.

THE USGS-CGS PRELIMINARY TIME-DEPENDENT SEISMIC HAZARD MODEL

The time-dependent hazard model presented in this paper is based on the time-independent, or Poissonian, 2002 national seismic hazard model and additional recurrence information for A-type faults that include: San Andreas, San Gregorio, Hayward, Rodgers Creek, Calaveras, Green Valley, Concord, Greenville, Mount Diablo, San Jacinto, Elsinore, Imperial, Laguna Salada, and the Cascadia subduction zone (figure 1). A-type faults are defined as having geologic evidence for long-term rupture histories and an estimate of the elapsed time since the last earthquake. A simple elastic dislocation model predicts that the probability of an earthquake rupture increases with time as the tectonic loading builds stress on a fault. Thus, the elapsed time is the first-order parameter in calculating time-dependent earthquake probabilities. However, other parameters such as static elastic fault interactions, visco-elastic stress-transfer, and dynamic stress changes from earthquakes on nearby faults will also influence the short-term probabilities for earthquake occurrence. In this paper we consider only the influence of the elapsed time since the last earthquake.

Over the past 30 years, the USGS and CGS have developed time-dependent source and ground-motion models for California using the elapsed time since the last earthquake (WGCEP, 1988, 1990, 1995 [led by the Southern California Earthquake Center], 1999, 2003; Cramer *et al.* 2000; Petersen *et al.* 2002, appendix A). The probabilities of occurrence for the next event were assessed using Poisson, Gaussian, log-normal, and Brownian passage time statistical distributions. Past working groups applied a value of about 0.5 ± 0.2 for the ratio of the total sigma to the mean of the recurrence distribution. This ratio, known as the coefficient of variation, accounts for the periodicity in the recurrence times for an earthquake; a coefficient of variation of 1.0 represents irregular behavior (nearly Poissonian) and a coefficient of variation of 0 indicates periodic behavior. For this analysis, we have applied the parameters shown in table 1 to calculate the time-dependent earthquake probabilities. The basic parameters needed for these simple models are the mean-recurrence interval (T-bar), parametric uncertainty (Sigma-P), intrinsic variability (Sigma-P and Sigma-T), and the year of the last earthquake. The parametric sigma is calculated from the uncertainties in mean displacement and mean slip rate of each fault (Cramer *et al.* 2000). The intrinsic sigma describes the randomness in the periodicity of the recurrence intervals. The total sigma for the log-normal distribution is the square root of the sum of the squares of the intrinsic and parametric sigmas. For this analysis we assume characteristic earthquake recurrence models with segment boundaries defined by previous working groups.

We calculated the time-dependent hazard using the 2002 WGCEP report (WGCEP 2003) for the San Francisco Bay area, the 2002 National Seismic Hazard and Cramer *et al.* (2000) models for the other faults in northern and southern California, and the Petersen *et al.* (2002) model for the Cascadia subduction zone. Members of the WGCEP reran the computer code that was used to produce the WGCEP (2003) report and provided an update to the time-dependent probabilities for the San Francisco Bay area for 1-, 5-, 10-, 20-, 30-, and 50-year time periods beginning in 2006.

The 2002 USGS seismic hazard model (Frankel *et al.* 2002) assumes that the Cascadia subduction zone ruptures either in a **M** 9.0 event or in a series of **M** 8.3 events. Paleotsunami data from the coast of Oregon and Washington indicate a recurrence of large to great earthquakes every 500 years (Petersen *et al.* 2002). For the Cascadia subduction zone, we applied a time-dependent model for a magnitude **M** 9.0 earthquake scenario using a mean recurrence of 500 years, an aperiodicity parameter of 0.5, and the date of the last earthquake of A.D. 1700. The 50-year time-dependent probability is about 14%, which is slightly higher than the Poisson probability of about 10% (Petersen *et al.* 2002). For the **M** 8.3 scenario, we assume that individual events rupture about 250 km of the 1,100-km length of the subduction zone and fill the entire zone every 500 years. We would need about four and one-half **M** 8.3 events to fill the entire subduction zone every 500 years. These parameters require that **M** 8.3 events occur about every 110 years, if we do not consider clustering. However, this rate seems quite high given that **M** 8.3 earthquakes have not been observed during the past 150–200 years of recorded history. Therefore, in this study we do not feel justified in increasing the time-dependent hazard for the **M** 8.3 scenario given the historic earthquake record, and we simply use the Poisson rate in our calculations. The **M** 9.0 and 8.3 models were equally weighted in the 2002 hazard model as well as in this time-dependent model.

The San Andreas (Parkfield segment), San Jacinto, Elsinore, Imperial, and Laguna Salada faults were all modeled using single-segment ruptures following the methodology of Cramer *et al.* (2000). Multisegment ruptures were allowed in the WGCEP 1995 model, but these were not incorporated in this time-dependent model.

We developed three southern San Andreas models that consider various combinations of the five segments of the southern San Andreas fault that were defined by previous working groups (Cholame, Carrizo, Mojave, San Bernardino, and Coachella) and three multiple-segment ruptures. In the time-dependent models, 11% of the occurrence rate is based on the Poisson model, and 89% is based on the time-dependent model, similar to the method applied in WGCEP (2003). For the time-dependent portion of the model, it is easier to define the single-segment time-dependent probabilities because there are published recurrence rates and elapsed times since the last rupture for these segments based on historical and paleo-earthquake studies (*e.g.*, WGCEP 1995). However, defining time-dependent multiple-rupture probabilities (cascades) is much more complicated.

The first time-independent model (T-I Model 1), assumes single-segment and multiple-segment ruptures with weights that balance the moment rate and that are similar to the observed paleoseismic rupture rates (Frankel *et al.* 2002, appendix A). Possible rupture models of the southern San Andreas include: (a) ruptures along five individual segments, (b) rupture of the southern two segments and of the northern three segments

(similar to the 1857 earthquake rupture), and (c) rupture of all five segments together. For each of the complete rupture models, the magnitudes of the earthquake were determined from the rupture area. Recurrence rates were assessed by dividing the moment rate along the rupture with this calculated magnitude. The single-segment rupture models were weighted 10% and the multisegment rupture models were weighted 90% (50% for submodel b and 40% for submodel c) to fit the observed paleoseismic data.

In the first time-dependent model (T-D Model 1), which is based on T-I Model 1, probabilities are calculated, as in previous working groups, using a log-normal distribution for the parametric sigmas listed in table 1. For the time-dependent portion of the model, we have adjusted the Poisson probabilities to account for the information from the time-dependent probabilities of single-segment events. Individual segments of the southern San Andreas fault have higher time-dependent probabilities than the corresponding Poisson probabilities (a probability gain); therefore, the multisegment rupture should also have higher time-dependent probabilities than the Poisson model. Since it is not known in advance what segment might trigger rupture of the cascade, this multisegment rupture probability is calculated using the weighted average of the probability gains from each of the segments involved in the rupture, where the weights are proportional to the 30-year time-dependent probability of each segment. We show an example containing two segments in appendixes B and C.

The second time-independent model (T-I Model 2) is also based on the 2002 national seismic hazard model (model 2) and considers characteristic displacements for earthquake ruptures. This model assumes two multiple-segment ruptures that are composed of segments from Cholame through Mojave (1857-type ruptures) and from San Bernardino through Coachella. In addition, single-segment ruptures of the Cholame and Mojave are considered. This model assumes that the Carrizo segment only ruptures in 1857-type earthquakes with a rate of 4.7×10^{-3} events/yr, based on paleoseismic observations. Therefore, this multisegment rupture accounts for 22 mm/yr of the total slip rate of 34 mm/yr (WGCEP 1995), given the earthquake rate and a 4.75 m characteristic slip on the Cholame segment. The remaining 12 mm/yr is taken up by single-segment ruptures of the Cholame segment. Using a single-segment magnitude of 7.3 and a 12mm/yr slip rate yields a single-segment recurrence rate for Cholame of 2.5×10^{-3}/yr. For the Mojave segment, the slip rate available after the slip from 1857-type ruptures is removed is 9 mm/yr. Using an earthquake with magnitude 7.4 (4.4 m/event) for single-segment rupture and a slip rate of 9 mm/yr yields a recurrence rate of 2.05×10^{-3} for a single-segment Mojave rupture. For the San Bernardino through Coachella rupture an **M** 7.7 earthquake with recurrence rate of 5.5×10^{-3} event/yr is consistent with the paleoseismic data. Inclusion of other ruptures on these segments leads to estimated recurrence rates that exceed the paleoseismic observations. The total moment rate of this model is 92% of the total predicted moment rate.

The second time-dependent model (T-D Model 2), which is based on T-I Model 2, accommodates the difference between the total segment time-dependent rupture rate (the time-dependent rate of all potential ruptures that involve that segment) and the corresponding multiple-segment rupture rate that involves that segment. The segment time-dependent probabilities for all ruptures combined are calculated the same way as for the first model and are shown in table 1. The Carrizo segment is assumed to rupture only in 1857-type events and its total segment time-dependent probability is the same as the time-dependent probability for the 1857-type events (following the partial cascades model in Petersen *et al.* 1996 and Cramer *et al.* 2000). We first calculate a time-dependent probability P_{ctotal} for any type of rupture scenario involving the Cholame segment (single-segment or 1857-type). Here we use the total recurrence rate derived from the time-independent calculation from Model 2. Next we calculate the time-dependent probability P_{1857} for 1857-type ruptures using the paleoseismic recurrence rate. The time-dependent probability of a single-segment Cholame rupture is derived from the total time-dependent rate (calculated from P_{ctotal}) subtracted from the rate of the 1857-type events (converted from P_{1857}). An example is shown in appendix C.

The time-dependent rate for the Coachella and San Bernardino segments rupturing together has to be the smaller of the two segment rates. In T-I Model 2, the San Bernardino segment is not allowed to rupture by itself. When the conditional probability weighting is applied, this rupture has to be allowed in order to accommodate the excess rate on this segment. Its time-dependent rate is the segment rate (converted from probability) subtracted from the event rate of the Coachella and San Bernardino segments rupturing together.

For the third model we have applied two rupture scenarios that are based on new (*i.e.*, post-2002) geologic data and interpretations: (1) single-segment time-dependent rates that were used in model 1 above and (2) two multisegment ruptures, the 1857-type rupture that includes the Carrizo, Chalome, and Mojave segments and the southern multisegment rupture that includes the San Bernardino and Coachella segments. The recurrence rates and elapsed time since the last earthquake for multisegment ruptures are based on geologic data shown in Weldon *et al.* (2004, figure 12). The five single-segment rupture models were weighted 10% and the two multisegment ruptures were weighted 90%, similar to the weighting in T-I Model 1. The multisegment earthquakes incorporate a recurrence time of 200 years (five events in 1,000 years) and elapsed time of 149 years for the 1857-type event and a recurrence time of 220 years (four events in 880 years) and elapsed time of 310 years for the southern two-segment rupture. In general the models of Weldon *et al.* (2004) are moment-balanced using slip rate. However, when we apply the 200- and 220-year recurrence intervals to the 1857-type (**M** 7.8) and southern multisegment rupture that includes the San Bernardino and Coachella segments (**M** 7.7), we obtain a moment rate that is about 80% of the other models. The reason for the lower moment is that the magnitude of the multisegment rupture is not specified in the Weldon *et al.* (2004) model. If the magnitude of the 1857-type rupture is

raised from **M** 7.8 to **M** 7.9 the updated model releases about the same moment as the other models and is moment-balanced. This slight magnitude adjustment would not change the hazard calculation significantly because ground motions from **M** 7.8 and **M** 7.9 earthquakes are very similar. Therefore, for model 3 we have maintained the **M** 7.8 magnitude in order to be consistent with the magnitudes used in other models, recognizing that the moment rate is a little lower as a result. Weldon *et al.* (2004) also show data that indicate variability in the southern extent of the 1857 ruptures and the northern extent of the southernmost multisegment rupture in the vicinity of the 1812 rupture. Therefore, we have also included an aleatory variability for the segment boundary near the southern end of the 1857 rupture and have not included the 1812 rupture as the date of the last event. We have developed time-independent (Poisson) and time-dependent models for these ruptures (T-I Model 3 and T-D Model 3). An example is calculated in appendix C.

The time-independent, or Poisson, hazard map of peak ground acceleration for 10% probability of exceedance in 30 years from the 2002 national seismic hazard model is shown in figure 2 and the corresponding time-dependent hazard map is shown in figure 3; the time-dependent probabilities are listed in table 2. The time-dependent map is developed from the WGCEP (2003) model for the San Francisco Bay area; the Cramer *et al.* (2000) model for the San Andreas (Parkfield), San Jacinto, Elsinore, Imperial, and Laguna Salada faults; and the Petersen *et al.* (2002) model for the Cascadia subduction zone. In addition, the southern San Andreas hazard was developed using T-D Models 1, 2, and 3 with equal weighting. The differences between the time-dependent and time-independent models are difficult to distinguish at the scale presented in figures 2 and 3. Therefore, we have developed a ratio map to highlight the differences (figure 4).

DISCUSSION AND CONCLUSIONS

In this paper we have presented both time-independent and time-dependent probabilities for several faults and statewide ground motion hazard maps for California that show the value of peak ground acceleration with a 10% probability of exceedance for a time period of 30 years starting in 2006. The time-dependent maps differ by about 10% to 15% from the time-independent maps near A-fault sources (figure 4). However, for most of California, located well away from the time-dependent sources, the ground motions are similar. The southern San Andreas fault, Cascadia subduction zone, and the eastern San Francisco Bay area faults generally have elevated hazard relative to the time-independent maps. This is because it has been quite a long time since the last earthquake—about 150 years since the 1857 **M** 7.9 Fort Tejon earthquake, more than 300 years since the 1700 **M** 9 Cascadia earthquake, and nearly 140 years since the 1868 **M** 6.8 on the southern Hayward fault. All of these faults are, most likely, in the latter half of their seismic cycles. The northern San Andreas fault, southern San Jacinto fault, and Imperial fault, on the other hand, have time-dependent hazard that is lower than the time-independent hazard due to the relatively short period since the 1906 (**M** 7.8) San Francisco earthquake, the 1968 (**M** 6.4) Borrego Mountain earthquake, and the 1971 Imperial Valley **M** 6.4 earthquake, which places these faults in the first half of their seismic cycles. Sites located well away from the A-faults are typically controlled by local faults, especially for high frequencies greater than 1 hz.

Three time-independent and corresponding time-dependent models that are proposed in this paper are based on characteristic earthquake recurrence models that have distinct segment boundaries; for T-D Model 3 we have allowed the end of the rupture to vary according to the geologic models. For the past 15 years WGCEP reports have all applied the characteristic model with fixed or slightly variable boundaries. Recent studies (*e.g.*, Weldon *et al.* 2004) suggest that other more random ruptures also fit the same geologic data constraining earthquake ruptures on the southern San Andreas fault. This implies that strict characteristic models should be relaxed in future time-dependent hazard calculations to account for this potential variability in source models. Variable rupture characteristics may not result in significant changes to the hazard at low frequencies (*i.e.*, long return periods), but could be considered in future WGCEP models.

Probabilistic hazard maps are used for making important risk mitigation decisions regarding building design, insurance rates, land use planning, and public policy issues that need to balance safety and economics. This map is the basis for the Working Group on California Earthquake Probability–Uniform California Earthquake Rupture Model version 1.0 (UCERF 1.0) and will be used to compare current 2006 methods with future, more complex, models. It is important that state-of-the-art science be incorporated in hazard maps that are used for public policy. Generally hazard products should be updated regularly as new information on earthquake recurrence and ground shaking becomes available from the science community. Research on such important hazard topics as recurrence time and rupture histories of prehistoric earthquakes, magnitude-frequency distributions for individual faults, and the effects of shallow and deep site conditions on ground shaking will improve these maps in the future.

ACKNOWLEDGMENTS

We acknowledge Bill Ellsworth and Ned Field for calculating the time-dependent rates of earthquakes for 2006–2036 using the 2002 working group model and Ken Rukstales for producing GIS maps for figure 1. Rob Wesson, Yuehua Zeng, Mark Stirling, Ned Field, and an anonymous reviewer provided helpful reviews of the manuscript.

REFERENCES

Abrahamson, N. A., and W. J. Silva (1997). Empirical response spectral attenuation relations for shallow crustal earthquakes. *Seismological Research Letters* **68** (1), 94–127.

Algermissen, S. T., and D. M. Perkins (1982). *A Probabilistic Estimate of Maximum Acceleration in Rock in the Contiguous United States*. USGS Open File Report 76-416.

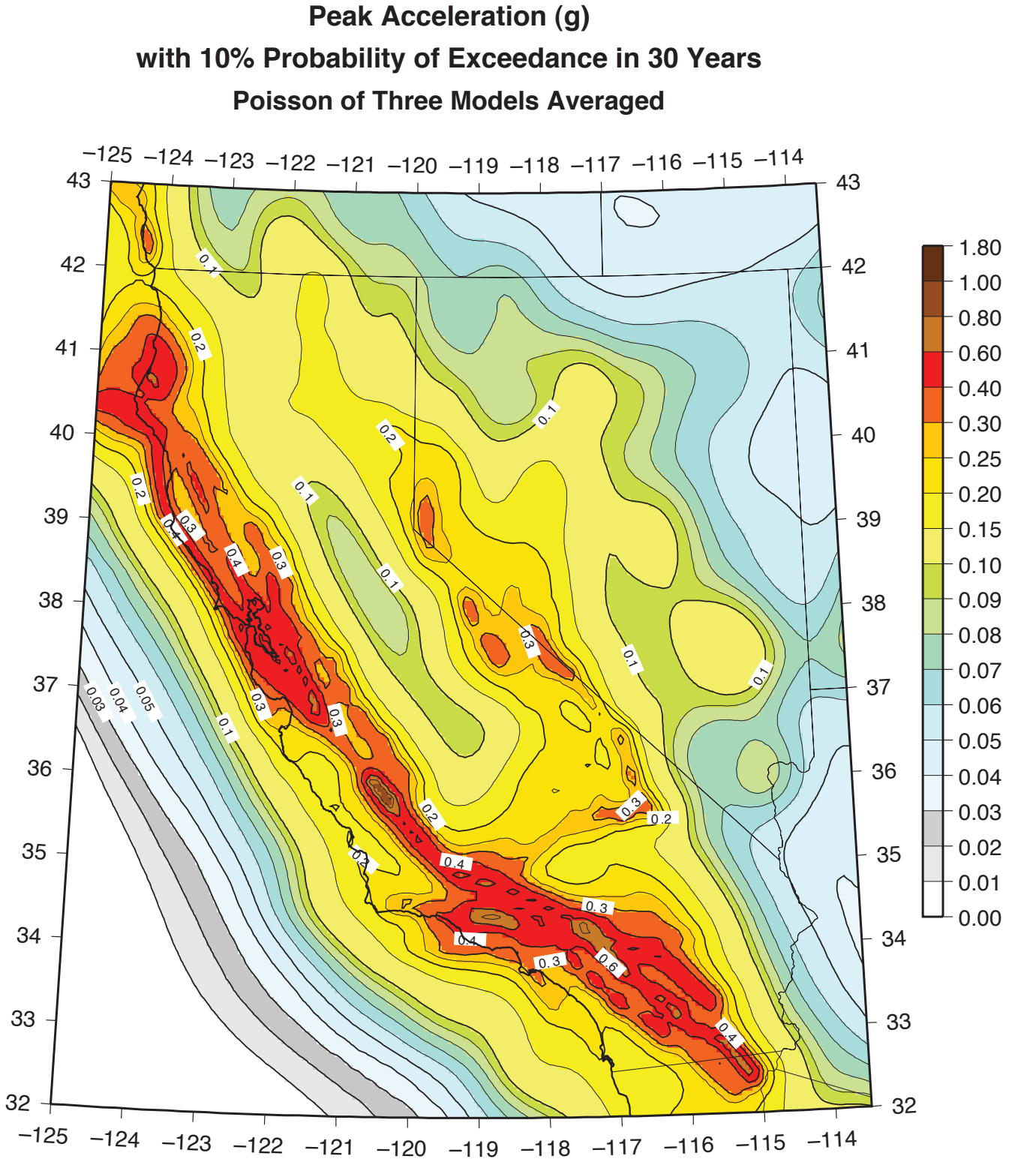

▲ **Figure 2.** Time-independent (Poisson) map for rock site condition and a 10% probability of exceedance in 30 years. This map was developed from the 2002 national seismic hazard model but also includes the new Poisson model for T-I Model 3.

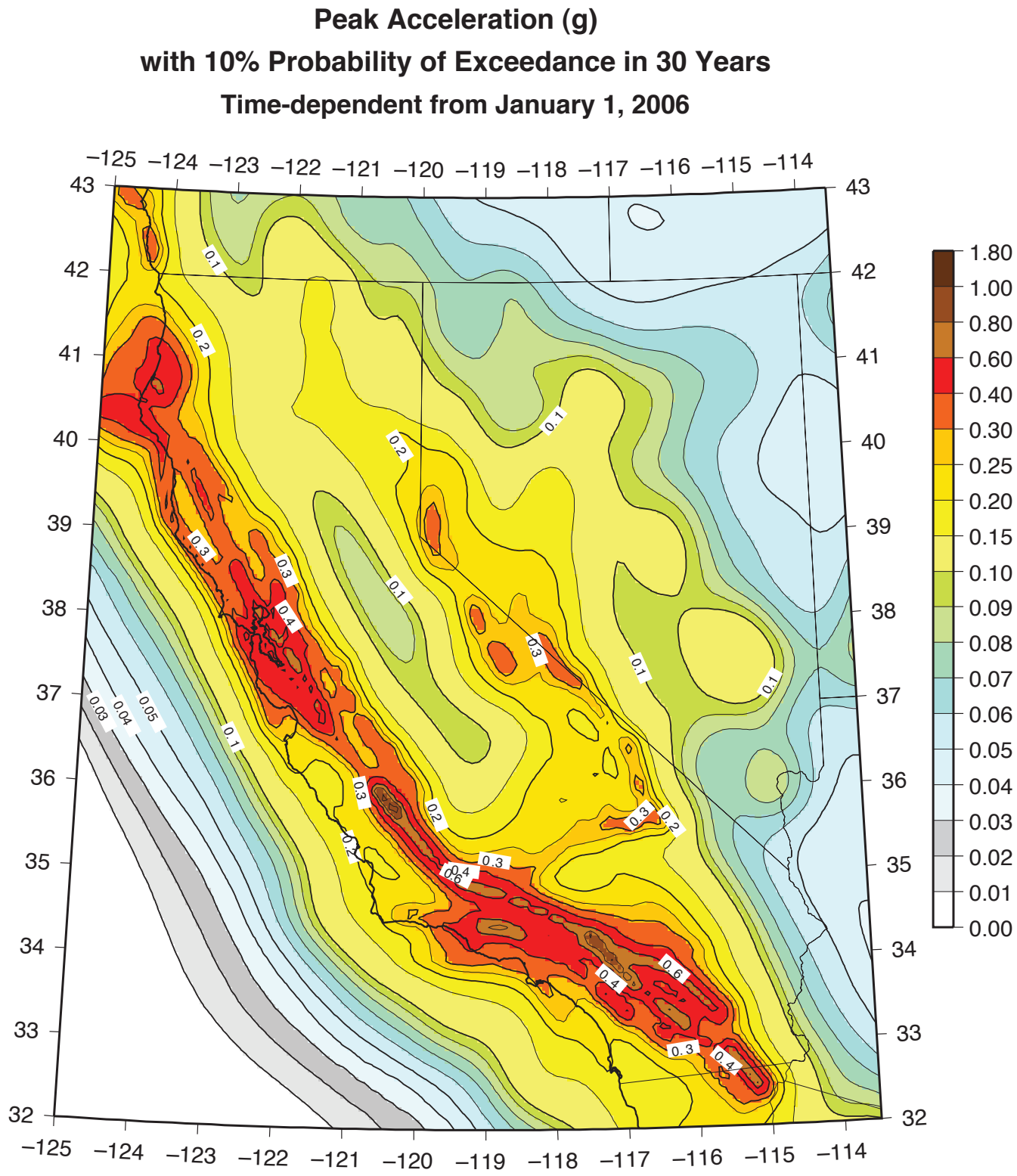

▲ **Figure 3.** Time-dependent map for rock site condition and a 10% probability of exceedance in 30 years. This map was developed by equally weighting three time-dependent models (T-D model 1, 2, and 3).

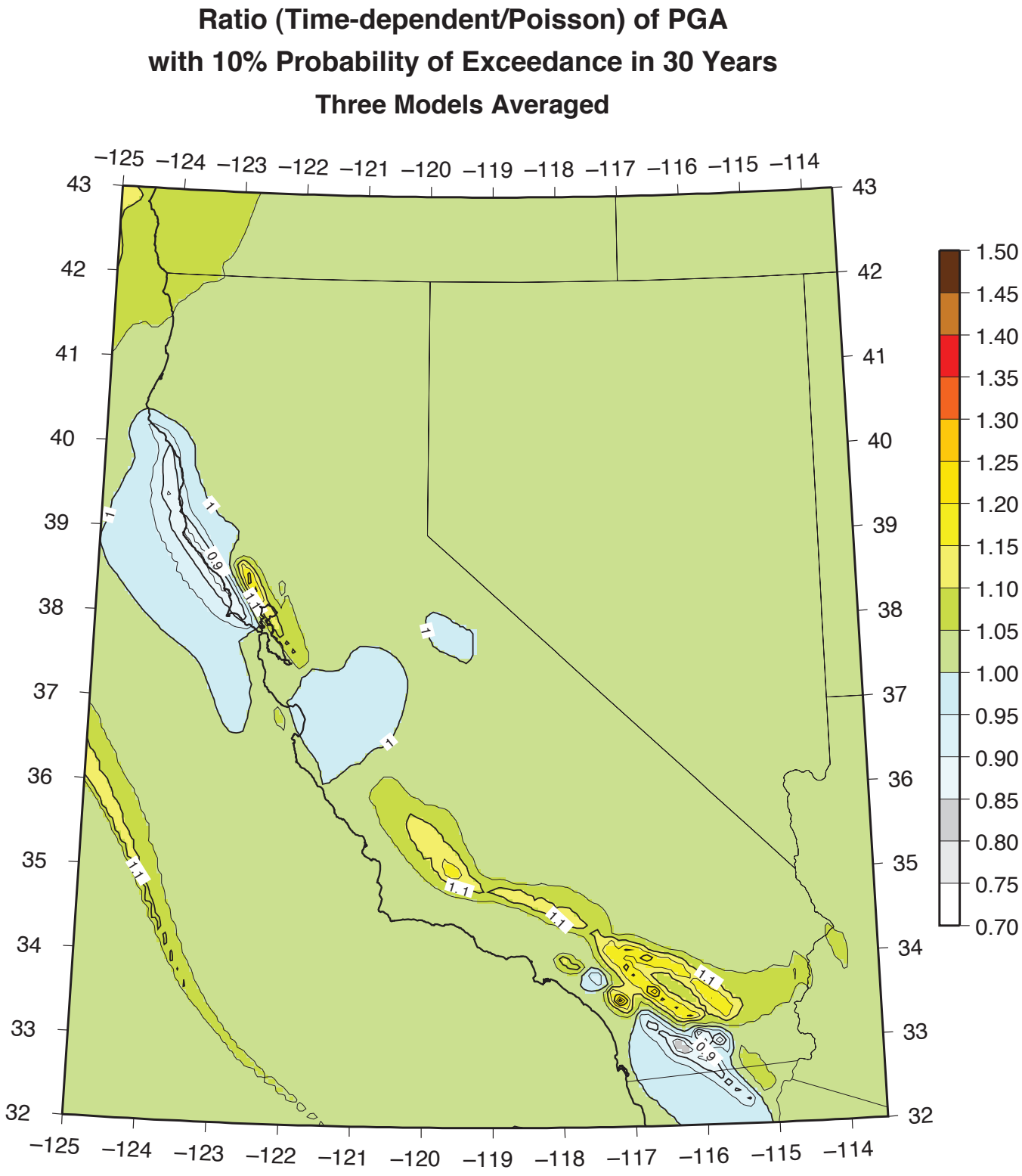

▲ **Figure 4.** Ratio of the time-dependent map (figure 3) and the time-independent map (figure 2) for rock site conditions and a 10% probability of exceedance in 30 years.

Atkinson, G. M., and D. M. Boore (2003). Empirical ground-motion relations for subduction zone earthquakes and their application to Cascadia and other regions. *Bulletin of the Seismological Society of America* **93**, 1,703–1,709.

Boore, D. M., W. B. Joyner, and T. E. Fumal (1997). Equations for estimating horizontal response spectra and peak acceleration from western North American earthquakes: A summary of recent work. *Seismological Research Letters* **68**, 128–153.

Campbell, K. W., and Y. Bozorgnia (2003). Updated near-source ground motion (attenuation) relations for the horizontal and vertical components of peak ground acceleration and acceleration response spectra. *Bulletin of the Seismological Society of America* **93**, 314–331.

Cramer, C. H., M. D. Petersen, T. Cao, T. R. Toppozada, and M. S. Reichle (2000). A time-dependent probabilistic seismic-hazard model for California. *Bulletin of the Seismological Society of America* **90**, 1–21.

Frankel, A. (1995). Mapping seismic hazard in the Central and Eastern United States. *Seismological Research Letters* **66** (4), 8–21.

Frankel, A., C. Mueller, T. Barnhard, D. Perkins, E. Leyendecker, N. Dickman, S. Hanson, and M. Hopper (1996). *National Seismic-Hazard Maps: Documentation June 1996*. USGS Open File Report 96-532.

Frankel, A. D., M. D. Petersen, C. S. Mueller, K. M. Haller, R. L. Wheeler, E. V. Leyendecker, R. L. Wesson, S. C. Harmsen, C. H. Cramer, D. M. Perkins, K. S. Rukstales (2002). *Documentation for the 2002 Update of the National Seismic Hazard Map*. USGS Open File Report 02-420.

Gardner, J. K., and L. Knopoff (1974). Is the sequence of earthquakes in southern California, with aftershocks removed, Poissonian? *Bulletin of the Seismological Society of America* **64**, 1,363–1,367.

Gutenberg, B., and C. F. Richter (1944). Frequency of earthquakes in California. *Bulletin of the Seismological Society of America* **34**, 185–188.

Petersen, M. D., W. A. Bryant, C. H. Cramer, T. Cao, N. S. Reichle, A. D. Frankel, J. J. Lienkaemper, P. A. McCrory, and D. P. Schwartz (1996). *Probabilistic Seismic Hazard Assessment for the State of California*. California Division of Mines and Geology Open-File Report 96-08, USGS Open File Report 96-706.

Petersen, M. D., C. H. Cramer, M. S. Reichle, A. D. Frankel, and T. C. Hanks (2000). Discrepancy between earthquake rates implied by historic earthquakes and a consensus geologic source model for California. *Bulletin of the Seismological Society of America* **90**, 1,117–1,132.

Petersen, M. D., C. H. Cramer, and A. D. Frankel (2002). Simulations of seismic hazard for the Pacific Northwest of the United States from earthquakes associated with the Cascadia subduction zone. *Pure and Applied Geophysics* **159**, 2,147–2,168.

Sadigh, K., C. Y. Chang, J. Egan, F. Makdisi, and R. Youngs (1997). Attenuation relationships for shallow crustal earthquakes based on California strong motion data. *Seismological Research Letters* **68**, 180–189.

Schwartz, D. P., and K. J. Coppersmith (1984). Fault behavior and characteristic earthquakes: Examples from the Wasatch and San Andreas faults. *Journal of Geophysical Research* **89**, 5,873–5,890.

Spudich, P., W. B. Joyner, A. G. Lindh, D. M. Boore, B. M. Margaris, and J. B. Fletcher (1999). SEA99: A revised ground motion prediction relation for use in extensional tectonic regimes. *Bulletin of the Seismological Society of America* **89**, 1,156–1,170.

Stirling, M., and M. Petersen (2006). Comparison of the historical record of earthquake hazard with seismic-hazard models for New Zealand and the continental United States. *Bulletin of the Seismological Society of America* **96**, 1,978–1,994.

Toppozada, T., D. Branum, M. Petersen, C. Hallstrom, C. Cramer, and M. Reichle (2000). *Epicenters of and Areas Damaged by M≥5 California Earthquakes, 1800–1999*. California Division of Mines and Geology map sheet 49.

Weldon, R., K. Sharer, T. Fumal, and G. Biasi (2004). Wrightwood and the earthquake cycle: What a long recurrence record tells us about how faults work. *GSA Today*, **14** (9), 8.

Working Group on California Earthquake Probabilities (WGCEP) (1988). *Probabilities of Large Earthquakes Occurring in California on the San Andreas Fault*. USGS Open File Report 88-398.

Working Group on California Earthquake Probabilities (WGCEP) (1990). *Probabilities of Large Earthquakes in the San Francisco Bay Region, California*. USGS Survey circular 1053.

Working Group on California Earthquake Probabilities (WGCEP) (1995). Seismic hazards in southern California: Probable earthquakes, 1994–2024. *Bulletin of the Seismological Society of America* **85**, 379–439.

Working Group on California Earthquake Probabilities (WGCEP) (1999). *Earthquake Probabilities in the San Francisco Bay Region: 2000 to 2030—A Summary Of Findings.* USGS Open File Report 99-517.

Working Group on California Earthquake Probabilities (WGCEP) (2003). *Earthquake Probabilities in the San Francisco Bay Region: 2002-2031*. USGS Open File Report 03-214.

Youngs, R. R., S. J. Chiou, W. J. Silva, and J. R. Humphrey (1997). Strong ground motion attenuation relationships for subduction zone earthquakes. *Seismological Research Letters* **68** (1), 58–73.

U.S. Geological Survey
Denver Federal Center
MS 966 Box 25046
Denver, Colorado 80225 USA
mpetersen@usgs.gov
(M.D.P.)
afrankel@usgs.gov
(A.D.F.)

California Geological Survey
801 K Street MS 12-31
Sacramento, California 95814 USA
tcao@consrv.ca.gov
(T.C.)

EQECAT Inc.
1030 NW 161st Place
Beaverton, Oregon 97006 USA
KCampbell@eqecat.com
(K.W.C.)

APPENDIX A

For this paper we calculated the time-dependent probabilities for time periods of 5, 10, 20, 30, and 50 years. For these calculations we have generally assumed a log-normal probability density function; however, the working group 2003 report used a Brownian passage time model that does not cause a significant difference from the log-normal distribution except for very long elapsed times since the previous earthquake. Following the WGCEP 1995 report we find that the density function $f(t)$ has the following form:

$$f_T(t) = \frac{1}{t\sigma_{\ln T_i}\sqrt{2\pi}} \exp\left\{\frac{-\left[\ln\left(t/\hat{\mu}\right)\right]^2}{2\sigma^2_{\ln T_i}}\right\}, \qquad \text{(A1)}$$

where μ is the mean, $\hat{\mu}$ is the median, $\sigma_{\ln T_i}$ is the intrinsic sigma, and t is time period of interest. If $\hat{\mu}$ and $\sigma_{\ln T_i}$ are known, then the conditional time-dependent probability in time interval $(t_e, t_e + \Delta T)$ is given by

$$P\left(t_e \le T \le t_e + \Delta t \mid T > t_e\right) = \frac{P(t_e \le T \le t_e + \Delta t)}{P(t_e \le T \le \infty)} \quad , \qquad \text{(A2)}$$

where t_e is the elapsed time and ΔT is the time period of interest. A Poisson process follows the rule: $P = 1 - \exp(-rT)$, where P is the Poisson probability, r is the rate of earthquakes, and T is the time period of interest. If we want to convert between probability P and rate r, then we can use the formula

$$r = -\ln(1 - P) / t. \qquad \text{(A3)}$$

We calculate the probability and annualize this rate using equation (A3).

APPENDIX B

If we denote the calculated time-dependent probabilities and time-independent (Poisson) probabilities for two single-segment rupture events as P_a^t, P_b^t, P_a^p, and P_b^p, the ratios $R_a = P_a^t / P_a^p$ and $R_b = P_b^t / P_b^p$ are sometimes called the probability gain or loss over the average Poisson probabilities. For a multisegment (cascade) event involving these two segments, we also define the probability gain or loss as $R_{ab} = P_{ab}^t / P_{ab}^p$, in which the Poisson probability P_{ab}^p is known. Since P_{ab}^p already accounts for the conditional probability of multisegment rupture, we further assume that the cascade event is triggered by independent rupture of one of the segments A or B. So we know that $R_{ab} = R_a$ if the cascade event starts from A and that $R_{ab} = R_b$ if it starts from B. Assuming segment A is more likely to rupture in some future time period than segment B, then $R_a > R_b$, and the chance of a cascade event occurring must be smaller than the chance of A rupturing but larger than the chance of B rupturing. Therefore, R_{ab} has to be smaller than R_a but larger than R_b if $R_a > R_b$ and vice versa. Considering that a cascade event can start from A or B with different likelihoods, we approximate R_{ab} by weighting R_a and R_b by P_a^t and P_b^t, their probabilities of rupture, resulting in the cascade event ratio $R_{ab} = (P_a^t R_a + P_b^t R_b) / (P_a^t + P_b^t)$. The physical basis for this type of weighting process is that the multisegment rupture has to originate from the segment that has the highest probability.

APPENDIX C

Example applications for calculating time-dependent rates:

Models 1 and 3

In this section we show how the annual occurrence rates for a multisegment rupture are calculated in models 1 and 3. For our first example, we calculate the rate of rupture that involves all five segments. The time-dependent 30-year probabilities for the five segments Coachella, San Bernardino, Mojave, Carrizo, and Cholame are 0.325, 0.358, 0.342, 0.442, and 0.512 assuming a log-normal distribution. The equivalent annual rates are calculated using the formula $r = -\ln(1 - p)/t$, where p is the segment time-dependent probability in t (30 years). This rate is divided by the Poissonian rate of the 2002 model and produces the probability gain for each segment. The gains for five segments are 1.141, 1.918, 1.065, 1.690, and 1.114. The weighted gain for this five-segment rupture is 1.384 [*i.e.*, (0.325 × 1.141 + 0.358 × 1.918 + 0.342 × 1.065 + 0.442 × 1.690 + 0.512 × 1.114 / (0.325 + 0.358 + 0.342 + 0.442 + 0.512)]. The final annual rate for this rupture is the Poissonian rate (0.00355) multiplied by this gain and the 2002 model weight (0.4), which is 0.00196 (*i.e.*, 0.00355 × 1.384 × 0.4).

For model 3, the cascading allows only 1857- and 1690-type events, and their recurrence times are 200 and 220 years respectively, which differs from the 2002 model. We follow the same steps as in the T-D Model 1 to calculate the time-dependent annual rates for the multisegment ruptures with the new Poissonian rates for multisegment events. After obtaining the time-dependent annual rates for the 1857 and 1690 type multisegment ruptures, we weight each of the Weldon *et al.* (2004) rupture scenarios included in the model.

Model 2

In 2002 T-I model 2, the Poissonian rates for the five segments are different from T-D Model 1. We apply these different mean recurrence times and the same elapse times and intrinsic and parametric uncertainties and calculate time-dependent 30-year probabilities and their equivalent annual rates as we did in model 1. These rates are 0.008260, 0.010336, 0.008908, 0.007396, and 0.011173 for the Coachella, San Bernardino, Mojave, Carrizo, and Cholame segments respectively. The Carrizo segment in T-D Model 2 only ruptures in 1857-type events, so the time-dependent annual rate for an 1857-type rupture is defined as the rate for the Carrizo segment (0.007396). The Cholame and Mojave segments are allowed in the 2002 T-I model to rupture independently (T-I Models 1 and 2). The time-dependent probability for the Cholame and Mojave segment events is their segment probability subtracted from the rate of 1857-type events or 0.003777 (*i.e.*, 0.011173 – 0.007396) for Cholame and 0.001512 (*i.e.*, 0.008908 – 0.007396) for Mojave ruptures. The time-dependent rate for Coachella and San Bernardino segments rupturing together has to be the smaller of the two segment rates or 0.00826 (< 0.011173). In the 2002 T-I model 2, the San Bernardino segment is not allowed to rupture by itself. But now the difference between the San Bernardino segment rate (0.010336) and the rate (0.008260) for San Bernardino and Coachella segments rupturing together defines the single-segment rupture on the San Bernardino segment, *i.e.,* (0.002076 = 0.010336 – 0.008260).